

Supernova Fallback: A Possible Site for the r-Process

Christopher L. Fryer^{1,2}, Herwig, Falk², Hungerford, Aimee⁴, and F.X. Timmes^{1,3}

ABSTRACT

The conditions for the leading r-process site candidate, neutrino-driven winds, can not be reproduced self-consistently in current supernova models. For that reason, we investigate an alternate model involving the mass ejected by fallback in a supernova explosion, through hydrodynamic and nucleosynthesis calculations. The nucleosynthetic products of this ejected material produces r-process elements, including those in the vicinity of the elusive 3rd peak at mass number 195. Trans-iron element production beyond the second peak is made possible by a rapid ($< 1ms$) freezeout of α particles which leaves behind a large nucleon (including protons!) to r-process seed ratio. This rapid phase is followed by a relatively long ($\gtrsim 15ms$) simmering phase at $\sim 2 \times 10^9$ K, which is the thermodynamic consequence of the hydrodynamic trajectory of the turbulent flows in the fallback outburst. During the slow phase high mass elements beyond the second peak are first made through rapid capture of both protons and neutrons. The flow stays close to valley of stability during this phase. After freeze-out of protons the remaining neutrons cause a shift out to short-lived isotopes as is typical for the r-process. A low electron fraction isn't required in this model, however, the detailed final distribution is sensitive to the electron fraction. Our simulations suggest that supernova fallback is a viable alternative scenario for the r-process.

Subject headings: Nuclear Reactions, Nucleosynthesis, r-process, Abundances, Stars: Supernovae: General

1. Introduction

Production mechanisms for elements heavier than iron, by fast (r-process) and slow (s-process) captures of neutrons, have been known for a long time (Cameron 1957, Burbidge

¹Department of Physics, The University of Arizona, Tucson, AZ 85721

²Theoretical Division, LANL, Los Alamos, NM 87545

³Applied Physics Division, LANL, Los Alamos, NM 87545

⁴Computer and Computation Sciences Division, LANL, Los Alamos, NM 87545

et al. 1957), yet finding conditions in Nature and understanding the physics that allow these mechanisms to robustly operate has been more elusive. The search for an r-process production site has proven especially difficult. The supernova wind model (see Qian & Woosley 1996 for a detailed description), invoking the neutrino-driven wind produced by the cooling proto-neutron star formed in a core-collapse supernovae, is the best-studied r-process mechanism. However, the wind scenario generally seem to require uncommon conditions (e.g. $> 2 M_{\odot}$ neutron star; Argast et al. 2004; Suzuki & Nagataki 2005) to achieve a reasonable r-process signature.

Difficulties with the wind mechanism have led to investigations about other possible sites for the r-process; the best-studied being the coalescence of two neutron stars (Freiburghaus 1999). Unfortunately, the low event rate of merging neutron stars appears to rule out binary coalescence as a primary production site (Argast et al. 2004). Most other mechanisms have been based on the suggestions by Qian & Woosley (1996) from changes in the neutrino/nuclear physics (e.g. neutrino oscillations - Qian et al. 1993) to magnetic fields (e.g. Suzuki & Nagataki 2005). In this paper we explore supernova fallback, yet another of Qian & Woosley (1996).

After the launch of a supernova explosion, some of the material initially ejected in the blast can decelerate and fall back onto the proto-neutron star. This “fallback” material was initially proposed by Colgate (1971) who argued that a rarefaction wave would catch the shock and the lack of pressure support would cause the shock to fall back onto the neutron star. Essentially, the material with ejecta velocities below the escape velocity will fall back onto the neutron star. Shigeyama, Nomoto, & Hashimoto (1988) and Woosley (1989) proposed a scenario where fallback occurs when the shock decelerates as it moves through the star. This deceleration sends a reverse shock through the star, decelerating the innermost material and causing it to accrete. This mechanism is strongest when the shock hits the hydrogen envelop, attaining its most dramatic deceleration. Simulations show that fallback occurs early (Fryer et al. 1999; MacFadyen et al. 2001), establishing that sub-escape velocity ejecta dominates fallback material (Fryer & Kalogera 2001). Indeed, Fryer & Heger (2000) found fallback in a disk in the first second after the launch of the explosion.

Although simulations of supernova explosions suggest that fallback occurs in all simulations, this is not yet the prevailing view among core-collapse theorists. Fallback is strongest when the explosion is weak and it may be that only for weak supernovae, $M \geq 20 M_{\odot}$, that the fallback mechanism can work (Fryer 1999). This does not preclude fallback as an r-process source! In fact, Argast et al. (2004) found that narrow ranges of massive stars can explain the entire r-process abundance pattern.

In this paper, we present the first calculations of the r-process based on hydrodynamic

simulations of fallback, the ejection of fallback material (§2), and detailed nucleosynthesis calculations of the ejecta (§3). Without tuning our initial conditions, we find that fallback leads to ejecta that carry abundance signatures characteristic for r-process, thereby demonstrating that ejecta from the fallback of material onto neutron stars is a viable r-process site.

2. Ejecta from Fallback

We have modeled the fallback material and ejection of a fraction of this material using the 2-dimensional Smooth Particle Hydrodynamics code described in Fryer et al. (1996). The neutron star is modeled as a $1.4 M_{\odot}$, 10 km hard surface emitting neutrinos. This code includes an equation of state valid from densities below 1 g cm^{-3} up to nuclear densities and a flux-limited diffusion neutrino transport scheme for 3 neutrino species (Herant et al. 1994). The mass and entropy of the ejecta depend upon a range of assumptions for the initial conditions: neutrino luminosity and energy and the accretion rate, angular momentum and composition of the infalling flow.

For this simulation, we modelled an early time ($< 50 \text{ s}$) fallback and added a neutrino flux of $2 \times 10^{51} \text{ erg s}^{-1}$ in electron neutrinos (with a mean energy of 10 MeV), and $1.6 \times 10^{51} \text{ erg s}^{-1}$ in electron anti-neutrinos (with a mean energy of 15 MeV). The results presented here do not depend sensitively on this choice of neutrino emission, as neutrino absorption is not the dominant force driving mass ejection. We also do not incorporate neutrino absorption in the presented nucleosynthesis calculations. That is, we do not use the electron fractions determined in the hydrodynamics calculation in the post-process nucleosynthesis calculation, but instead set the electron fraction to a constant value: $Y_e = 0.5$ for our standard calculation.

The accretion rates from current fallback simulations predict a range of mass inflow rates. Piston-driven explosions using the 1-dimensional stellar evolution code KEPLER (Fryer et al. 1999) found accretion rates ranged from nearly 10^4 - $10^5 M_{\odot} \text{ y}^{-1}$ over a brief time (accreting roughly $0.1 M_{\odot}$) for low mass progenitors down to $10^4 M_{\odot} \text{ y}^{-1}$ for an extended period for a $25 M_{\odot}$ star (accreting over $1 M_{\odot}$). MacFadyen et al. (2001) studied a $25 M_{\odot}$ progenitor with a range of explosion energies with accretion rates between 10^3 and $10^4 M_{\odot} \text{ y}^{-1}$ for strong explosions producing neutron star remnants to fallback rates as high as $10^6 M_{\odot} \text{ y}^{-1}$ that ultimately produce black holes. For our simulations, we used the fairly normal $10^4 M_{\odot} \text{ y}^{-1}$ value, representing a snapshot in time of the fallback in a supernova explosion.

The angular momentum in stellar cores, and hence fallback, is still quite uncertain. Heger et al. (2000, 2004) find the angular momentum in the core at the time of collapse

ranges from $10^{15-17} \text{ cm}^2 \text{ s}^{-1}$. In our calculation, we have assumed an angular momentum at the low end of this range $10^{15} \text{ cm}^2 \text{ s}^{-1}$. With such a low angular momentum, the accreting material does not form a centrifugally supported disk. However, the angular momentum does affect the flow, as we shall see at the end of this section. For high angular momenta, the infalling material will form a disk and disk outflows will drive most of the ejecta.

Lastly, we had to choose the composition of the fallback material. It has long been believed that the ejecta from core-collapse will be neutron rich (Arnett & Truran 1970) and many of the successful explosion models have ejected neutron-rich ($Y_e < 0.5$) material (e.g. Herant et al. 1994). Indeed, it was in an effort to remove these neutron rich ejecta that Colgate (1971) began to study fallback. Some recent calculations (e.g. Pruet et al. 2005) have found that the neutrinos reset the electron fraction leading to ejecta that are proton rich ($Y_e > 0.5$). To reset the electron fraction, the neutrino-driven wind must play a dominant role in driving the explosion (more likely in weak explosions with considerable fallback). We have used two initial compositions, one with $Y_e=0.5$ (all ^{56}Ni), more consistent with the most recent results, and one with $Y_e = 0.49$ (^{56}Ni with some ^{52}Fe), closer to past results.

With this 2-dimensional smooth particle hydrodynamics code and these initial conditions, we followed the evolution of the fallback for 3.5 s. The results for our $Y_e=0.5$ simulation at 0.82 s are shown in figure 1. Material crashes down onto the neutron star and is shocked, in some cases to entropies above $250 k_B \text{ nucleon}^{-1}$. Some of the material bubbles up and is driven off the neutron star by the energy released from the accreting material. Recall that material accreting onto the neutron star releases roughly $10^{20} \text{ erg g}^{-1}$. A small amount of accreting material can drive off 100 times its mass with ejecta velocities of $10,000 \text{ km s}^{-1}$ if the cooling is inefficient (because of the high temperature dependence of neutrino emission, this is often the case) and if you have some means of transporting energy out (e.g. viscous heating). This can occur because the infalling matter is only marginally bound. The potential energy is converted to kinetic and ultimately thermal energy during the infall, but the infalling matter remains only marginally bound throughout the infall (if cooling is inefficient, energy is conserved). If it can get a small amount of energy from its neighboring matter, it can become unbound. In our simulation, roughly 25% of all our accreting material is ejected with velocities greater than the escape velocity. The efficiency at which material is ejected depends on the angular momentum of the infalling material, neutrino cooling and neutrino heating. That there is ejecta is not a surprise, and the nature of this ejecta has been studied over a range of conditions. In the limit of high angular momentum and an absorbing boundary (i.e. black hole accretion disk), these outflows are well-studied: see Blandford & Begelman (1999) for a review. With a hard surface boundary, such as we would expect from our central neutron star, we expect outflows even at low angular momenta (Fryer et al. 1996).

The bubbling up ejecta from fallback expands and cools quickly through adiabatic expansion. Some matter shocked to temperatures above 10^{10} K can cool down to $2\text{--}4 \times 10^9$ K on millisecond timescales. But as these bubbles push against the additional fallback material, the expansion, and hence cooling, slows. This produces a simmering phase that is important for nucleon captures and the r-process. Although the rapid temperature drop and simmering phase should be generic features of matter ejected in fallback, the exact temperatures at which these two phases occur depends upon the initial conditions. Unfortunately, the yields depend sensitively on these temperatures. The dependencies on these different physical effects will be studied in detail in a later paper. For this paper, we focus on testing whether fallback ejecta can provide a viable r-process. It is the material with velocities greater than the escape velocity that we study in detail with our nuclear network.

3. Nucleosynthesis of Ejecta from Fallback

The thermodynamic histories of 6617 particles ($\sim 25\%$ of the particles in the collapse) that reached escape velocity were post-processed with a 3304 isotope network. The temperature and density histories of this material can be highly non-monotonic and is not sufficiently described by a simple adiabatic expansion or wind ansatz. The reaction rates were taken from experiment whenever possible, from detailed shell-model based calculations (Fisker et al. 2001) and from Hauser-Feshbach calculations (Rauscher & Thielemann 2000). Separation energies were taken from a combination of experiment (Audi & Wapstra 1995), the Hartree-Fock Coulomb displacement calculations of Brown et al. (2002) and theoretical estimates (Möller et al. 1995). The influence of thermal effects on weak decays was estimated from the Fuller et al. (1982). The reaction network was integrated with the semi-implicit, variable order algorithms described in Timmes (1999). Our reaction network features a nuclear statistical equilibrium (NSE) calculation to determine the abundances when the temperature exceeds 10^{10} K. This increases computational efficiency by over an order-of-magnitude, while producing very little discontinuity upon either entering or leaving NSE.

Figure 2 shows the stable isotope distribution attained by the 6617 particles that reach escape velocity as the black circles. This calculation assumed that every particle had an initial composition characterized by $Y_e=0.5$. For nearly all of the trajectories of interest the temperature goes above 10^{10} K and memory of the exact initial composition is forgotten except for its Y_e . Particles that populate the region around the $A=195$ peak are mainly produced by a three-step operation. A rapid freezeout as a result of rapid expansion causes a persistent disequilibrium between free nucleons and abundant alpha particles (Meyer 2002) followed by a relatively long simmering phase $\sim 2 \times 10^9$ K with proton and neutron mass

fractions $\sim 3 \times 10^{-3}$.

The flows that populate the region near $A=195$ stay initially close to the valley of beta stability. The nuclei mass is driven up past the neutron-closed shell at $N=82$ by an irregular, alternating succession of neutron and proton captures. This phase after α freeze out and before proton freeze out can be thought of as rapid proton and neutron capture process, hence the “rpn-process”. Figure 3 shows the trajectory of a single particle that produces elements near the $A=195$ peak along with snapshots of its isotopic abundances. The matter of this particle is shocked to temperatures well beyond 1 MeV. Panel three (lower left) shows the nucleosynthesis situation towards the end of this rpn-process phase. Then, at $t = 0.172$ s for this particular particle, protons freeze out, and the remaining neutrons are captured on a time scale of a few ms, driving the flow out to short half lives that are characteristic for the r-process.

Although the flows stay initially relatively close to the valley of beta stability, this material synthesizes r-process and not s-process elements. Figure 2 shows the solar abundance distribution, and the solar r-process component. Our distribution does not show some typical signatures of canonical s-process, including large abundances of ^{138}Ba and ^{208}Pb . Our models produce several elements, including Ba, Pb and Hg, which have a significant s-process contribution in the solar distribution. However, in our distribution the s-only isotopes are absent, which is another indication that our mechanism will not lead to s-process distribution. In addition, our global Ba/Eu ratio in the total ejected material is $[\text{Ba}/\text{Eu}] = -0.2$, which in observed stars would be taken as a clear indication of a r-process signature.

Although the existence of a $A \sim 195$ peak in our simulations shows the potential of fallback ejecta as an r-process site, our current simulation is far from reproducing the solar r-process signature. The yields from our simulation produce peaks that are wider and at slightly higher masses than observed. One reason for this could well be the uncertainties in the beta decay rates. Engel et al. (1999) have found that more accurate calculations of the beta decay rates lead to shorter half-lives, which cause the third peak to occur at lower mass. Such a shift might make our peaks more nearly match the observed data (see also Farouqi et al. 2005). Jordan & Meyer (2004) have more generally altered nuclear rates and found that the exact yield depends sensitively on this rates. So the differences between our results and the observed data may be resolved, at least partially, by uncertainties in the nuclear rates. The differences can also be resolved (as Meyer 2002 has already pointed out), by altering the exact value of the electron fraction. 1% variations in the electron fraction can change the yield from a clear r-process signature ($Y_e=0.495$) to a proton-rich yield ($Y_e=0.505$).

Our simulations of the ejecta from supernova fallback suggest the potential of this site to produce heavy elements in supernovae. Rapid cooling followed by a simmering phase allows

rapid proton and neutron captures with a final neutron burst to produce heavy elements, even with $Y_e \approx 0.5$. But we are far from reproducing the exact r-process yields. To determine if fallback is Nature's chosen site for r-process element production, we must include the time evolution of the electron fraction for each individual particle. Future work will also study the dependence of the yields on the fallback structure: accretion rate, angular momentum (which can drastically change the nature of the outflows), neutrino luminosity of the neutron star and initial electron fraction. A range of these values can occur in one supernova explosion. By studying the nucleosynthesis we may be able to derive more complete and realistic r-process yields for a given supernova explosion.

Acknowledgments We thank Al Cameron, Andy Davis, George Jordan, John Cowan, Brad Meyer, Hendrik Schatz, and Jim Truran for pragmatic discussions. This work was funded in part under the auspices of the U.S. Dept. of Energy, and supported by its contract W-7405-ENG-36 to Los Alamos National Laboratory, by a DOE SciDAC grant DE-FC02-01ER41176.

REFERENCES

- Arlandini, C., Käppeler, F., Wisshak, K., Gallino, R., Lugaro, M., Busso, M., & Straniero, O. 1999, *ApJ*, 525, 886
- Arnett, W.D. & Truran, J.W. 1970, *ApJ*, 160, 959
- Anders, E., & Grevesse, N. 1989, *Geochim. Cosmochim. Acta*, 53, 197
- Blandford, R.D. & Begelman, M.C. 1999, *MNRAS*, 303, L1
- Audi, G. & Wapstra, A.H. 1995, *Nucl. Phys. A*, 595, 409
- Argast, D., Samland, M., Thielemann, F.-K., & Qian, Y.-Z. 2004, *A&A*, 416, 997
- Burbidge, E.M., Burbidge, G.R., Fowler, W.A., Hoyle, F. 1957, *Rev. Mod. Physics*, 29, 547
- Brown, B.A., et al. 2002, *Phys. Rev. C*, 65, 5802
- Cameron, A.G.W. 1957, *AJ*, 62,9
- Colgate, S.A. 1971, *ApJ*, 163, 221
- Engel, J., Bender, M., Dobaczewski, J., Nazarewicz, W., and Surman, R. 1999, *PRC*, 60, 014302

- Farouqi, K., Freiburghaus, C., Kratz, K.-L., Pfeiffer, B., Rauscher, T., & Thielemann, F.-K. 2005, *Nuc. Phys. A* 758, 631
- Fisker, J. L., et al. 2001, *At. Data Nucl. Data Tables*, 79, 241
- Freiburghaus, C., Rembges, J.-F., Rauscher, T., Kolbe, E., Thielemann, F.-K., Kratz, K.-L., Pfeiffer, B., Cowan, J.J. 1999, *ApJ*, 516, 381
- Fryer, C.L., Benz, W., & Herant, M. 1996, *ApJ*, 460, 801
- Fryer, C.L., Colgate, S.A., & Pinto, P.A. 1999, *ApJ*, 511, 885
- Fryer, C.L. 1999, *ApJ*, 520, 650
- Fryer, C.L. & Heger, A. 2000, *ApJ*, 541, 1033
- Fryer, C.L. & Kalogera, V. 2001, *ApJ*, 554, 548
- Fuller, G.M., Fowler, W.A., & Newman, M.J. 1982, *ApJ*, 252, 715
- Herant, M., Benz, W., Hix, W.R., Fryer, C.L., Colgate, S.A. 1994, *ApJ*, 435, 339
- Jordan, G.C.,IV, & Meyer, B.S. in *The r-Process: The Astrophysical Origin of the Heavy Elements and Related Rare Isotope Accelerator Physics*, proceedings of the first Argonne/MSU/JINA/INT RIA Workshop held in January, 2004, at the University of Washington, USA. Edited by Yong-Zhong Qian, Ernst Rehm, Hendrik Schatz and Friedrich-Karl Thielemann. ISBN 981-256-032-7. Published by World Scientific Publishing Company, Singapore, 2004, p.157
- MacFadyen, A.I., Woosley, S.E., Heger, A. 2001, *ApJ*, 550, 410
- Meyer, B.S. 2002, *PRL*, 89, 1101
- Moller, P., Nix, J.R., Myers, W.D., & Swiatecki, W.J. 1995, *At. Data Nucl. Data Tables*, 59, 185
- Pruet, J., Woosley, S.E., Buras, R., Janka, H.-T., Hoffman, R.D. 2005, *ApJ*, 623, 325
- Qian, Y.-Z., Fuller, G.M., Mathews, G.J., Mayle, R.W., Wilson, J.R., & Woosley, S.E. 1993, *Phys. Rev. Lett.*, 71, 1965
- Qian, Y.Z., & Woosley, S.E. 1996, *ApJ*, 471, 331
- Rauscher, T. & Thielemann, F.-K. 2000, *At. Data Nucl. Data Tables*, 75, 1

Shigeyama, T., Nomoto, K., & Hashimoto, M. 1988, *A&A*, 196, 141

Suzuki, T.K., & Nagataki, S. 2005, *ApJ*, 628, 914

Timmes, F.X. 1999, *ApJS*, 124, 241

Woosley, S.E. 1989, *NY Acad. Sci. Ann.*, 571, 397

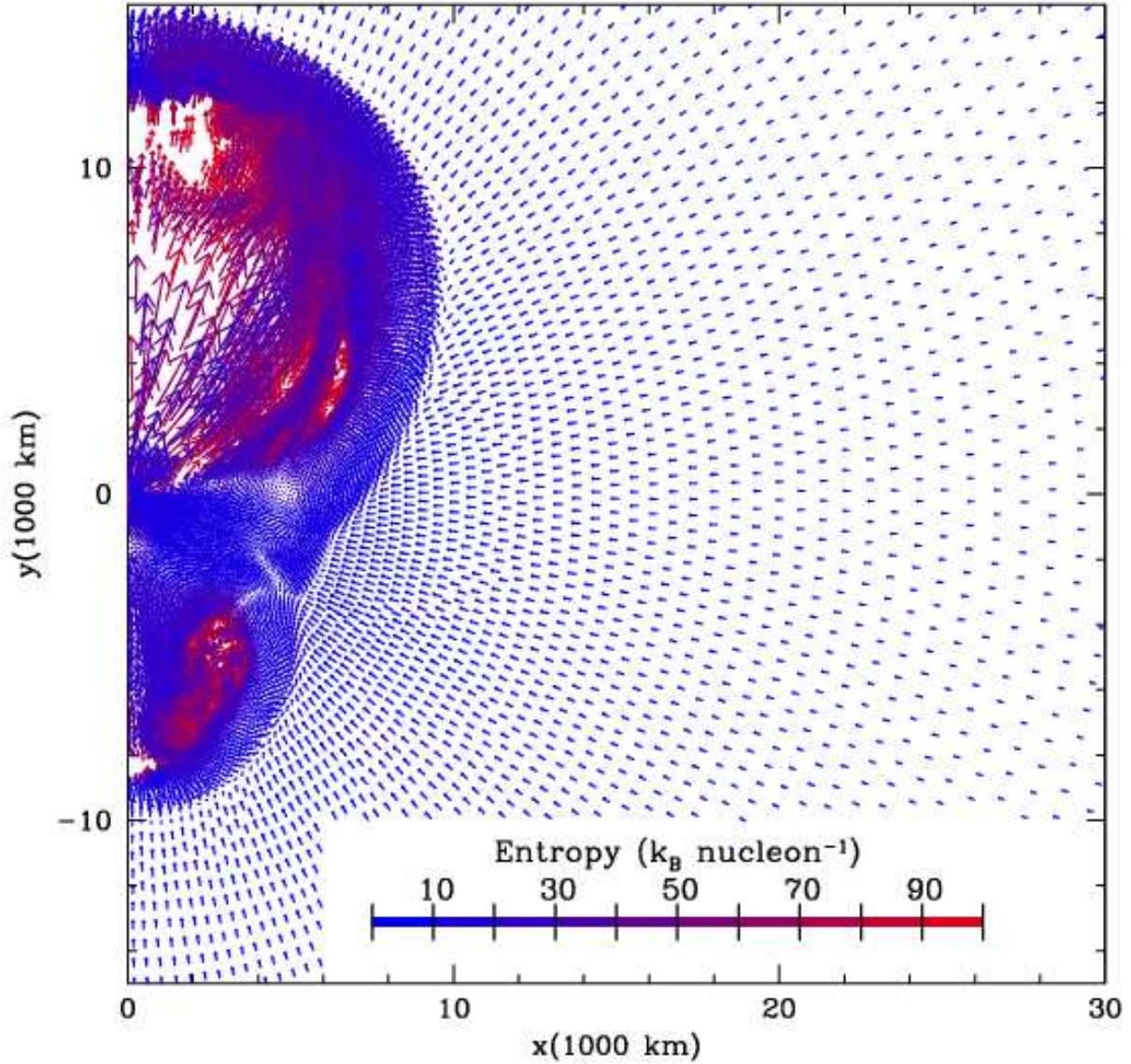


Fig. 1.— Accretion and mass ejection in supernova fallback 0.82s after initial fallback. Each point denotes particle position in the x - y plane of the 2-dimensional smooth particle hydrodynamics simulation where the y -axis is the axis of symmetry (set to the angular momentum axis of the fallback). The vectors denote velocity direction and magnitude (length of vector). The colors show entropy in units of Boltzmann constant per nucleon.

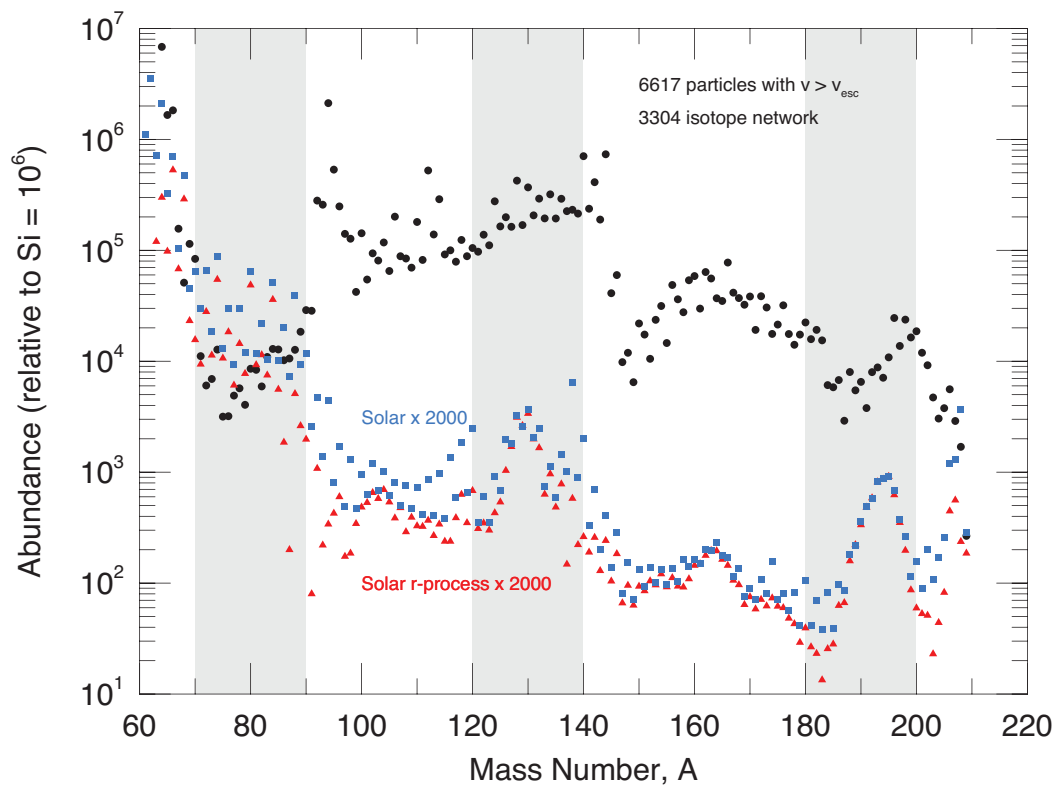


Fig. 2.— Abundance pattern of the stable isotopes for all the particles that achieved escape velocity (black circles). The calculation assumes all particles had an initial composition characterized by $Y_e=0.5$. The x-axis is the atomic mass number. The y-axis is the logarithm of the model abundance, normalized to an elemental silicon abundance of 10^6 . The Anders & Grevesse (1989) total solar abundance pattern is shown as the blue squares with r-process yields shown as red triangles.

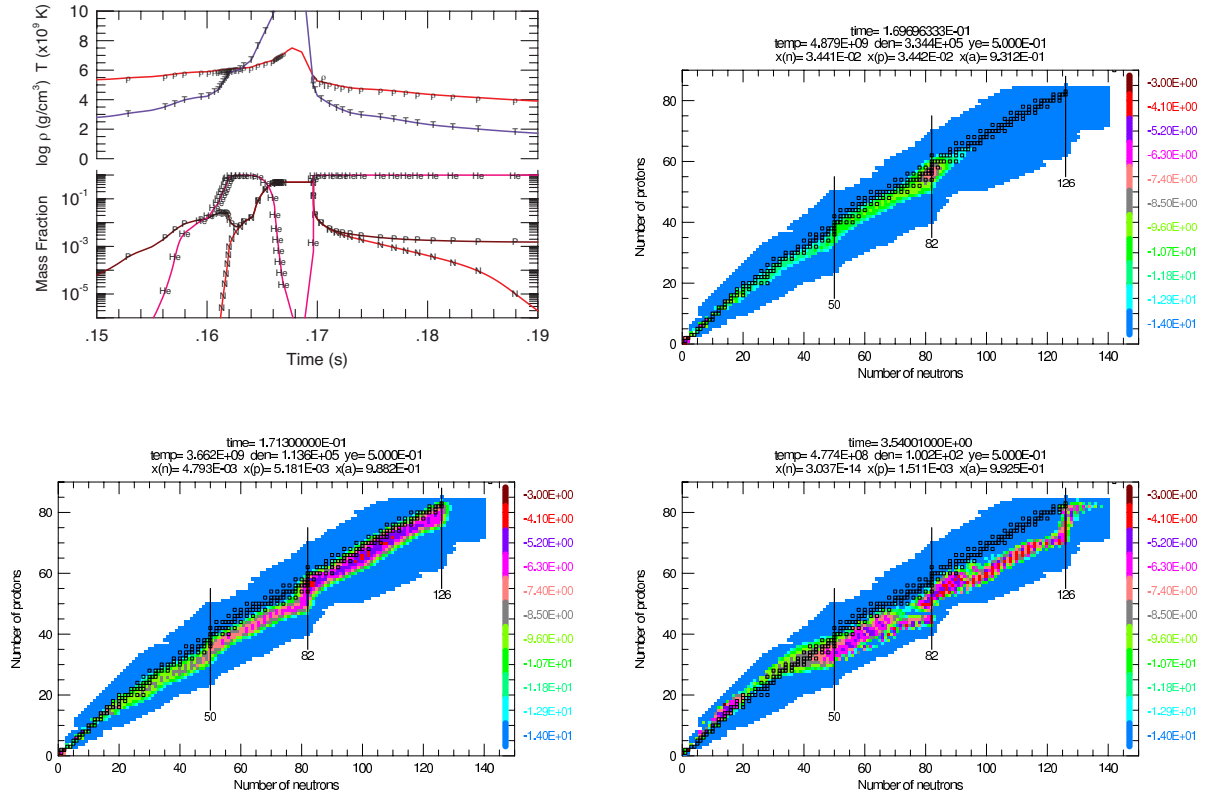


Fig. 3.— Evolution of the temperature, density, and neutron, proton and alpha abundances for one specific ejected particle. The sharp drop in temperature makes the neutrons and protons fall into disequilibrium with the alpha particles, leaving free neutrons and protons to capture onto heavy elements. We also show the element abundance at 3 different snapshots in time: 0.170 s, 0.171 s and 3.5 s. At 0.17 s, the material has just fallen from high temperatures down to a few times 10^9 K. The heavy elements center around the neutron numbers of 82. In the next 10 ms, rapid neutron and proton capture drive this material up to neutron numbers of 126. After this time, the temperature is too cool to allow proton capture, but neutron capture continues to drive the elements neutron rich, producing an r-process-like signature.